PRELIMINARY TESTING OF A PROPORTIONAL COUNTER FOR NEUTRON SPECTROSCOPY WITH HELIUM - 3

JOHN N. GREEN

UCRL-8274

UNIVERSITY OF CALIFORNIA
Radiation Laboratory
Berkeley, California

Contract No. W-7405-eng-48

PRELIMINARY TESTING OF A PROPORTIONAL COUNTER FOR NEUTRON SPECTROSCOPY WITH HELIUM-3

John N. Green

April 21, 1958

Submitted in partial fulfillment
of the requirements for the degree of
MASTER OF SCIENCE
IN
PHYSICS

United States Naval Postgraduate School
Monterey, California

Printed for the U. S. Atomic Energy Commission

PRELIMINARY TESTING OF A PROPORTIONAL COUNTER FOR NEUTRON SPECTROSCOPY WITH HELIUM-3

by

John N. Green

This work is accepted as fulfilling
the thesis requirements for the degree of

MASTER OF SCIENCE

IN

PHYSICS

from the

United States Naval Postgraduate School

PRELIMINARY TESTING OF A PROPORTIONAL COUNTER FOR NEUTRON SPECTROSCOPY WITH HELIUM-3

John N. Green

Radiation Laboratory
University of California
Berkeley, California

April 21, 1958

ABSTRACT

The He^3 (n, p)T reaction can be utilized in a proportional counter for neutron-energy determination in the region 100 kev to 1 Mev. This has already been demonstrated and the reaction cross section in this energy region has been measured with a counter. For practical application of the counter as a spectrometer, such as in health physics work, it is desirable to increase the counter efficiency. A proportional counter utilizing an anticoincidence ring to reduce wall effect has been constructed for this purpose. Some preliminary tests of the proposed system are described.

ACKNOWLEDGMENTS

This work was conducted under the guidance of Dr. Roger W. Wallace at the University of California Radiation Laboratory as part of the Special Physics curriculum of the U. S. Naval Postgraduate School, and done in part under the auspices of the U. S. Atomic Energy Commission.

The counter vessel was designed by Dr. Wallace and much of the construction was done by Robert Cence.

The author wishes to thank all members of Dr. Burton J. Moyer's Health Physics Group for their assistance during the course of the work.

Table of Contents

List of Illustrations and Tables

CHAPTER I

INTRODUCTION

The detection of neutrons and especially the measurement of their energy have from the first attempts presented a more difficult problem than for the other common nuclear particles. This is because the usual methods depended on effects resulting from the charges of the particles. The experiments by Dee in which he investigated the ionization produced in air in a cloud chamber irradiated by fast neutrons[1] were reported at the same time as Chadwick's announcement of the discovery of the neutron. Dee concluded that, if the neutron interacts with atomic electrons at all, the process produces not more than one ion pair per three meters of the neutron's path.

If we accept an arbitrary description of neutron energy, E_n, as intermediate neutrons: 1 kev to 500 kev, fast neutrons: 0.5 Mev to 10 Mev, then we may say in general that the predominant reaction of intermediate neutrons with nuclei is elastic scattering, and that in the fast range many other reactions appear, the most important of which is inelastic scattering[2]. Hydrogen- or methane-filled ionization chambers or proportional counters became an important method of detecting fast neutrons because the neutron can impart practically all of its energy to a proton in a head-on collision, and the recoil proton is then the particle causing the action of the counter. However, a determination of the neutron energy spectrum by the recoil method requires a thin radiator and a double collimation--first of the neutron beam and then of the recoil protons--resulting often in too low an efficiency. Theoretically, the second collimation may not be necessary because the neutron spectrum can be obtained from the recoil spectrum by differentiation, but this leads to large errors since we are effectively taking the differences of numbers of about the same size. Nuclear emulsions and organic scintillation counters have become very important detectors in neutron spectroscopy, especially for neutron energies above 1 Mev.

For energies below 1 Mev it became apparent that exothermic nuclear reactions might be useful for neutron spectroscopy. New methods were especially needed in health physics applications, where any schemes requiring collimation are automatically ruled out. Fast neutrons are of major concern to health physicists because of the difficulty of shielding against them, and their large relative biological effectiveness[3]. In 1946 Feld proposed that a proportional counter utilizing the (n, p) reaction might be useful for neutron spectroscopy in the 10- to 1000-kev range, with the advantage over recoils of detecting lower energies and making collimation unnecessary[4]. He considered the most promising reactions at that time:

$$N^{14}\ (n, p)C^{14},$$

$$Cl^{35}\ (n, p)S^{35}.$$

However, as he expected, these do not very well fulfill the first of the general requirements, which might be listed as follows:

(1) The reaction cross section should be fairly large and its variation with neutron energy smooth and free from resonances in the energy region of interest (and accurately known).

(2) The Q value of the reaction should be small, because $(E_n + Q)$ is the total energy measured by a counter, and for accuracy E_n cannot be too small a fraction of the total.

(3) There should be no low-lying excited states of the residual nucleus to cause an ambiguity in the energy of the reaction particles.

We can look for these requirements to be met over appreciable ranges only in light nuclei, in which the energy levels are more widely spaced, avoiding resonances and excited states. Also, for small Q values appreciable penetration of the Coulomb barrier for (n, p) or (n, α) charged-particle reactions would be limited to light nuclei.

Two (n, α) possibilities are

$$Li^{6}\ (n, \alpha)T,$$

$$B^{10}\ (n, \alpha)Li^{7}.$$

The first has a large Q (4.78 Mev) and a resonance at E_n = 0.27 Mev. The second, widely used for thermal neutron detection, has an excited state and fairly large Q values (2.79 and 2.31 Mev).

With supplies of helium-3 becoming more available and a likely possibility being $He^3(n, p)T$, helium-3-filled proportional counters came under consideration. In 1950 Coon showed that the cross section in the 1-Mev region was about 1 barn[5], comparable to the scattering cross section of hydrogen. The thermal cross section for this reaction is large (5400 ± 300 barns)[6]. These types of reaction cross sections obey the 1/v law for a wide range, but intermediate neutrons may depart from the 1/v law.

Some work on helium-3-filled proportional counters has been done by Batchelor and others at Harwell, England[7]. They used a small amount of helium-3 admixed with xenon or krypton as the counting gas and stopping gas to reduce wall effect. Also, a small amount of carbon dioxide was added to stabilize the multiplication process. In their final filling the pressure of krypton used was 164 cm of mercury. Since they found that, for E_n = 1 Mev, a pressure of 8 atmos of krypton is required to reduce the wall effect to 10%, they set up a computer program to correct for wall effect. Their work remeasured the neutron cross section in the range 120 kev to 1 Mev more accurately than previously, showing a much flatter energy dependence than the 1/v law.

They also pointed out a basic source of ambiguity in energy determination other than counter defects. As we show in Chaper VIII, the maximum recoil energy of a He^3 nucleus is $E_{He3} = 3/4\ E_n$. The true energy counts run from Q for $E_n = 0$ to $E_n + Q$. Thus, for $3/4\ E_n = Q$, the recoil spectrum begins to overlap the reaction spectrum. On the basis of Batchelor's value of Q as 770 kev, this means that ambiguities exist if neutrons of greater energy than 1.03 Mev are present. The scattering cross section up to about 20 Mev is comparable in size to the reaction cross section of interest, but of course only a fraction of those neutrons scattered deliver a large

portion of their energy to the He^3 recoils. In any case, the presence of high-energy neutrons reduces the accuracy.

Gaseous counters have notoriously low efficiency, and as helium-3 has become more plentiful and less expensive, it seems worthwhile to investigate the feasibility of increasing the counting rate by increasing the quantity of helium-3 in the counter. As we go to higher pressures, special problems arise, such as the demands for gas purity, higher voltages, and better insulation[8]. Also, the container must be more massive, and proper consideration should be given to the effects of the masses upon the spectral distribution of the neutrons, primarily caused by inelastic collisions (transparency correction). For these reasons it would be desirable to use helium-3 alone as the primary filling, utilizing it for the counting and stopping action. However, we soon find it very difficult to decrease wall effect to a reasonable value by helium-3 pressure alone because stopping powers decrease with lower atomic numbers. For instance, the following ranges of a 5.3-Mev alpha particle at one atmosphere have recently been measured[9]:

helium--21 cm,
krypton--3.0 cm,
xenon--2.2 cm.

For this reason it is desirable at the same time to determine the practicality of reducing the wall effect by surrounding the sensitive volume of the counter with an anticoincidence ring.

Since helium-3 is quite valuable, a fairly elaborate filling system must be devised to insure no loss of gas in filling and subsequent recovery. The purity requirements are not so great as in noble gas scintillation counting, in which a small amount of contaminant such as oxygen or other polyatomic gases may completely quench the useful scintillation property, but some purification arrangements will probably be needed in the filling system to achieve good energy resolution and to remove impurities which inevitably get in to the gas during filling and recovery. It is important that the

loss of helium-3 be kept small during the purification process. Purification procedures for noble gases using metallic calcium have been applied successfully for some time in removing all electro-negative impurities, nitrogen, hydrogen, and to a lesser degree carbon dioxide[10]. Also, the method of physical adsorption of impurities in an activated charcoal trap cooled to liquid nitrogen temperatures has been used successfully in a helium-3 system, and has the advantage of greater ease and convenience[11]. However, it appears there may be a special problem due to the radioactive background from tritium contamination of helium-3, and this problem is increased by using higher helium-3 pressure.

It was felt that useful information about these two techniques, (a) using helium-3 as the detecting medium and primary counting gas and (b) reducing wall effect with an anticoincidence ring, could be obtained by testing a counter with a filling of ordinary helium. The natural abundance of helium-3 is about 0.00013, so that it is not ordinarily noticeable. Owing to the large cross section at thermal energies, it can be detected in tank helium by use of a nuclear reactor as a source of neutrons, and this has been suggested as a way of surveying world helium supplies for helium-3 content[12]. Because it is a double-magic-number nucleus, He^4 is very stable, and the detection of neutrons in a helium-filled counter is due to the recoil alpha particles. Helium-3 and helium-4 have the same electronic configuration, and we can obtain information about the counting characteristics of one by experimenting with the other.

CHAPTER II

COUNTER SYSTEM

A method of reducing wall effect in proportional counters is to detect the particles that escape from the sensitive volume and exclude them from the measurements. To accomplish this it is desirable that the walls of the main counter be transparent and completely surrounded by transparent-walled counters in anticoincidence. The feasibility of Geiger-Mueller counters with transparent walls -- so that wall thickness would not limit the radiation to that above a minimum-- was investigated in 1944, and it was found that symmetrically placed wires could approximate a cylinder[13]. Single counters of triangular type were constructed with good results. However, when two such counters were placed close together, there was a deleterious effect due to distortion of the field at the central wire. Better results were obtained with a regular hexagonal shape.

COUNTER CONSTRUCTION

A counter has been constructed in which a layer of gas surrounding the main counter is in effect turned into a separate detecting device by a circular array of wires. The geometry is shown in Figs. 1 and 2. The inner circle of wires, grounded to the cylinder, serves as the cathode for the main counter and as the inner cathode wall for the ring counter. In the outer circle of wires alternate wires serve as cathode and counting wires for the ring counter. Since there are 36 wires in each circle, we effectively have the main counter surrounded by 18 separate counters.

An arrangement similar to this, referred to as a "wall-less counter", has been applied to low-energy beta spectroscopy and proved to be a practical instrument[14]. As pointed out, this prevents escaping high-energy particles from having an effect on the low-energy end of the spectrum, but the effective sensitive volume now depends on energy. However, inaccuracies because of this circumstance will

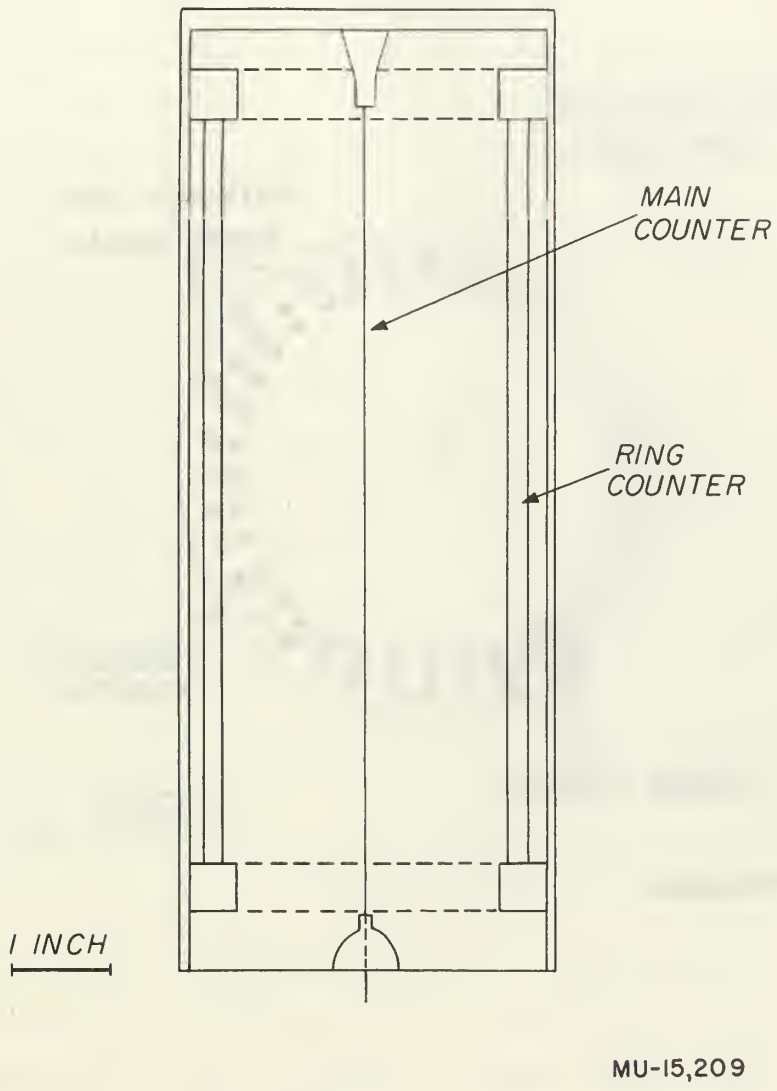

Fig. 1. Arrangement of counter.

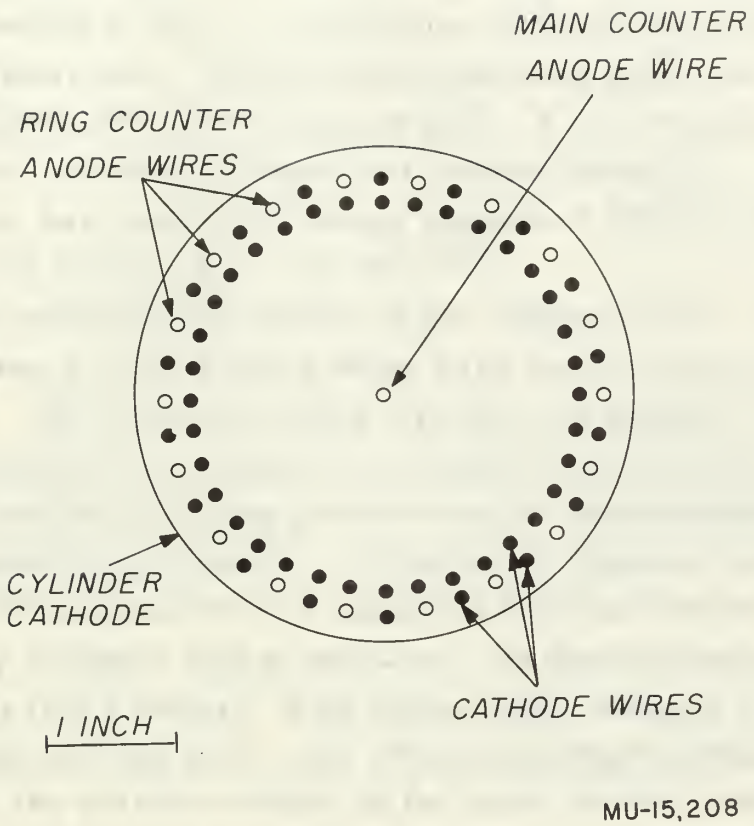

Fig. 2. Cross section of counter wiring.

be much less than from uncorrected wall effect. Another application of this type of counter geometry is the so-called "Giles telescope" neutron spectrometer[15]. In this arrangement the counter is long and narrow, and neutrons are collimated along the long axis. The requirement of a thin radiator is obviated by using gas recoils and the anticoincidence method to prevent registration of pulses that recoil oblique to the chamber axis. Monoenergetic neutrons then have a pulse-size distribution with a well-defined peak. A recent application of this scheme, utilizing hydrogen and propane fillings at various pressures, has resulted in energy spreads of 10% for neutron energies from a few hundred kev to 10 Mev[16].

Some of the constructional details of our counter follow. The counter cylinder has 1/16-inch-thick brass walls and is 4 inches in outside diameter. The total gas volume less the inlet piping is 1.93 liters. The vessel has been pressure- and leak-tested with helium at 20 atmospheres, making operating pressures up to 10 atmospheres possible within safety requirements. All wires are stainless steel of 3-mil diameter. The central wire is supported by kovar insulators and is electrically available only at the base. Its length between thickened supports is 8.5 inches. If we assume that, owing to a fall-off in field strength near the ends, only 90% of this length defines the sensitive volume, the sensitive volume of the main counter is 888 cc. The ring-counter anode wires and all cathode wires are each strung from a continuous piece of stainless steel wire and threaded through holes in $\frac{1}{2}$-inch-thick lava insulators at top and bottom, the anode wire system being electrically available through another kovar at the base. A major drawback to this method of stringing is the difficulty of repair in case of wire breakage. The volume defined by the ring counter is 600 cc.

The anticoincidence ring also cancels out particles that enter the counter from the outside or are emitted owing to contamination of the brass walls. Korff says a well-cleaned surface should emit 0.36 alpha particle per cm^2 per hour within a factor of ten[17], and

Sharpe gives 0.09 alpha particle per cm^2 per hour for commercial brass[18]. In normal operation the counter will probably not be sensitive to single secondary electrons knocked from the walls by gamma rays, but unwanted counts due to pile-up will be more likely in the ring counter, where the density of secondary electrons will be greater. A proportional counter with walls of copper tubing 1/32 inch thick has been used for counting gamma rays of energy up to 1.6 Mev[19]. The gamma-ray attenuation "tenfolding length" is approximately 60 g/cm^2 for all materials in the energy region where Compton scattering is the most important process[20]. This extends from less than one to several Mev for all elements. Multiplying by density, we find our brass wall is 1.34 g/cm^2 thick. The tenfolding length converted to a 1/e length is 26.1 g/cm^2. We have $\exp(-1.34/26.1) = 95\%$, therefore about 5% of all gamma rays impinging on the counter wall will be converted to secondary electrons. Of course, many of these electrons will be absorbed in the wall before reaching the counter gas, but gamma-ray counting efficiency would be reasonably high if the counter were operated at high gas multiplication.

The voltage at which a counter under given conditions is operated determines the gas multiplication. For a given counter Rossi and Staub have shown the functional relationship of multiplication[21] to be

$$M = M\left(\frac{V}{\ln \frac{b}{a}}, \quad Pa\right),$$

where

a = wire radius,
b = cathode radius,
P = gas pressure,
V = voltage across counter.

Since multiplication usually takes place in a cylindrical region of small diameter near the wire, we might assume our two counter systems identical for purposes of figuring multiplication, except for

the difference in ln b/a. The multiwire potential problem would be very difficult to compute, but if we take an average b value for one of the ring-counter wires (averaged over measurements to the inner circle of wires, to an adjacent wire in same ring, or to the wall), for the ring counter we obtain b/a = 225 and for main counter b/a = 1000. The ratio of the logarithms is 1.27, therefore for the same value of gas multiplication, this indicates that the main counter should have a higher voltage by a factor of 1.27. Of course, the determining factor on multiplication of the ring counter will be to make it as sensitive as possible in order to detect all particles that leave the main counter, but not so sensitive that a large number of background counts keep the desired counts from the main counter gated out.

ELECTRONIC CIRCUITRY

A block diagram of the electronic circuitry used with the counter is given in Fig. 3. The blocks below the dotted line complete the neutron-spectrometer system, but investigation of the operation of the system was made without this by scaling both coincidences and anticoincidences. A list of units actually used is given in Table I. One channel of the dual-channel variable gate and delay unit can be used for the variable-gate block, and the use of this unit for the pulse-shaping function could be replaced by simpler electronic circuitry. This unit is very useful, however, for experimenting with different values of discriminator setting and of delay and length of output pulses. If two pulses arrive at the pulse-shaping block at about the same time, we want to insure that there is no anticoincidence pulse to gate the pulse-height analyzer on. To do this we delay channel No. 1 slightly so that the channel No. 2 output pulse will definitely be at the coincidence unit before the channel No. 1 pulse arrives. Also, channel No. 2 pulse is made longer so that the coincidence unit will see it during the entire time that it sees the channel No. 1 pulse. The count on Scaler 1 + 2 indicates the number

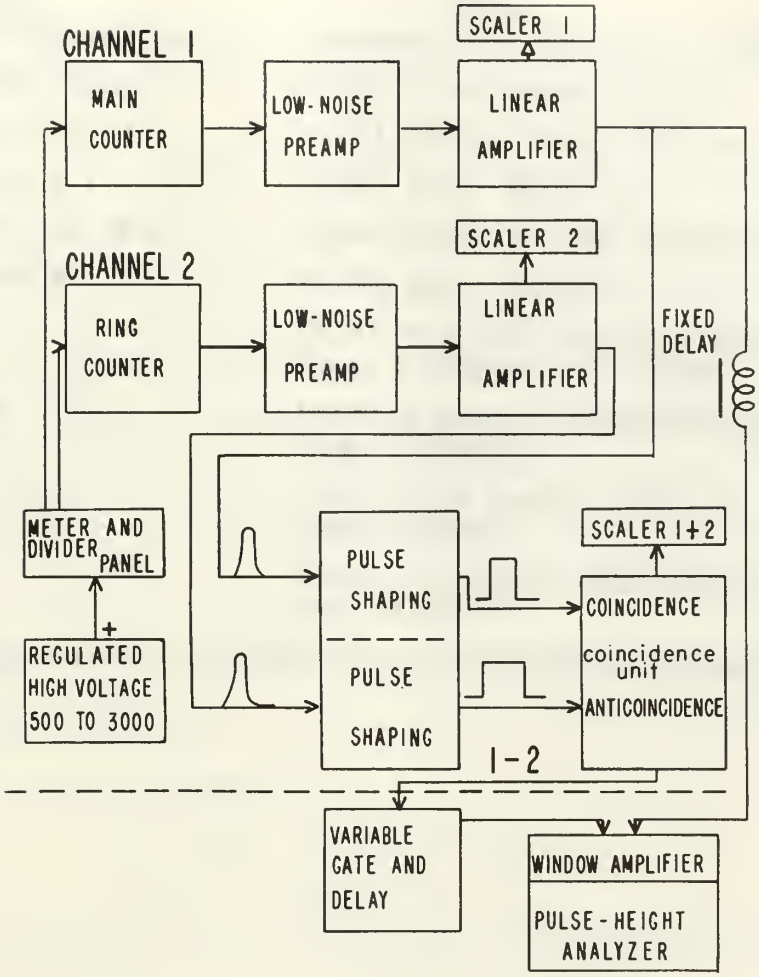

Fig. 3. Block diagram of counter electronic circuitry.

Table I. Units used in counter electronic circuitry.

Function	Unit
Regulated High Voltage Supply	Northern Scientific Co., ser. # 1
Meter and Divider Panel	UCRL 3 kv Divider Panel
Linear Amplifier, ch. # 1	UCRL Mod 5, Dwg. IX5334
Preamplifier, ch. # 1	UCRL Dwg. IX4353D
Linear Amplifier, ch. # 2	UCRL Mod. 3, Dwg. 2T4404
Preamplifier, ch. # 2	UCRL Dwg. 3T2393
Pulse Shaping	UCRL Variable Gate and Delay Unit Dwg. 2T8084F and 2T8154
Coincidence Unit	UCRL 8 Channel Quadruple Mixer Dwg. 3T5894-1
Scaler 1 + 2	UCRL 1024 Scaler, Mod. 2 Dwg. 3T8934
Scaler 1, 2	UCRL 2 Channel 1024 Scaler, Mod. 1 Dwg. 4T6895

of pulses from channel No. 1 not registered by the pulse-height analyzer. The versatile variable gate and delay unit, used with one input pulse and in conjunction with the coincidence unit, can also be used as a single-channel pulse-height analyzer if desired.

IONIC MOTION

With this size of counter one may have to worry about the time lag between formation of the pulse by the main counter and by the ring counter when ionization occurs close to the edge of the main counter. We can compute the travel time for ions if we know the mobility and how drift velocity depends on mobility and the field. Sharpe has developed convenient equations for computing ionic motion in chambers[18]. In general, in cylindrical or spherical fields, the field is

$$\epsilon = \frac{V r^{-n}}{\ln y} ,$$

where

$y = b/a$

r = radius,

V = voltage across counter,

and for a cylinder $n = 1$.

An ion crosses the system from one electrode to the other in a time given by

$$T = [a^{np+1} (y^{np+1} - 1)] / [(np+1) K (V/\ln y)^p] ,$$

where $p = \frac{1}{2}$ for electrons and 1 for ions in the equation relating drift velocity w to mobility K,

$$w = K\epsilon^p .$$

We are concerned with the time for an electron to travel across the counter because most of the pulse is formed near the wire owing to the concentration of the field at the wire whether there is multiplication or operation as an ion chamber. If we take a case of $V = 1000$ volts, $P = 2.5$ atmospheres of helium, and use Sharpe's value of

$K = 3.5 \cdot 10^4$ $cm^{3/2}/\sqrt{volt}$ - $sec\sqrt{atmos}$, we find for electrons $T = 7.55$ μsec. However, we expect that the mobility of a helium–carbon dioxide mixture may easily be greater by a factor of ten, based on the way CO_2 increases the drift velocity of electrons in other noble gases. This is explained for argon on the basis of the Ramsauer effect and the high first excitation potential for argon, 11.5 volts, in comparison with the low excitation levels in a CO_2 molecule[10]. The first excitation potential of helium is even higher, 19.77 volts. Extensive work has been done on collection times in argon, krypton, and xenon, and it is reported that once a fraction of one percent of CO_2 is added, the effect of original polyatomic impurities in a noble gas may be assumed insignificant[22]. The transit time computed above is reduced by the same factor as that by which the mobility is increased, and should not be too long for the coincidence requirements.

The transit time for a He^+ ion in pure helium to cross the system from wire to wall, computed for the same conditions as for the electron and on the basis of a mobility of 10.8 $cm.^2/volt\text{-}sec\text{-}atm.$ is 1850 μsec. This time is not too important, since the pulse can be shortened by shortening the amplifier time constant.

CHAPTER III

ENERGY RESOLUTION

A discussion of energy resolution depends on the complete theory of proportional-counter action. This has been well covered in several books and articles[10, 17, 18, 21, 23, 24, 25, 26]. The attempt here is to point out important factors concerning the energy resolution of this particular counter, using developments from any of the basic sources but modifying the terminology as necessary in order to be consistent.

INHERENT LIMITATIONS

Inherent fluctuations in a proportional counter are from (a) the number of ion pairs released by monokinetic radiation, and (b) the size of the avalanche each ionization electron produces. From theoretical work based on the assumption that the first was a Poisson distribution (it was found experimentally to be smaller than this) and expanded upon experimentally, it was shown that relative variance of total size of avalanche is approximately given by

$$Vp/(m_A m_O)^2 \approx 1/m_0 \qquad \text{(III-1)}$$

where

V_p = variance (mean square deviation) of size of avalanche,
m_0 = mean of number of ions initially liberated,
m_A = mean of number of ions produced in avalanche by one electron.

We note that this inherent spread is no longer a significant factor at the energies at which we will be working because in the 1-Mev energy range and at an assumed mean energy to produce an ion pair of 30 ev, m_0 is greater than 10^4. These theories were useful, and experiments were done down in the kev region where m_0 was a smaller number. For our magnitude of m_0, the relative variance would be around 0.01%. Since experience has shown that the relative spread of pulse height (relative standard deviation of pulse height from a monokinetic radiation) is at least 1% or 2% (owing to mechanical defects of

a counter or defects in gas filling) at these energies, the inherent spread is not a significant factor. The mean energy per ion pair, which determines m_0, is expected to be practically constant over the $(E_n + Q)$ range. This may not be true in very pure helium, in which the mean energy has been measured as 41.3 ev, in contrast to 29.7 ev when a small fraction of another gas is present. A possible explanation on the basis of charge exchange and the metastable states of helium is given by Sharpe with reference to experimental findings[18].

NEGATIVE-ION FORMATION

An important gas defect is negative-ion formation due to electron attachment to a gas molecule. It does not occur in pure noble gases nor in N_2, H_2, CO, CO_2, or CH_4. However, it is likely to occur in the collisions of electrons with the halogens, O_2, or water vapor. In the development of Eq. (III-1) the following equation was derived for the case where a fraction h' of ionization electrons reaches the wire without forming negative ions:

$$\frac{V_p'}{(h'm_A m_0)^2} = \frac{V_0}{m_0^2} + \frac{1}{m_0}\left(\frac{1.68}{h'} - 1\right), \qquad \text{(III-2)}$$

where V_0 = variance of number of ions initially liberated. For $h' = 1$ (no negative-ion formation), this equation leads to the previous approximation that relative variance is about $1/m_0$ when we use an experimental result that $V_0 = m_0/3$. That is, the relative variance is approximately

$$\frac{1}{m_0}\left[\frac{1}{3} + \left(\frac{1.68}{h'} - 1\right)\right].$$

(A bibliographical review on the development of Eqs. (III-1) and (III-2) is given in Reference 26).

Thus, for accuracy in low-energy work it is recommended that the gas be purified to remove negative-ion-forming impurities. However, since the factor in brackets in the expression for relative

variance is multiplied by the reciprocal of m_0, we expect that in our case the purification requirements may not be so stringent. This can be roughly checked by an approximate expression[18] for the concentration C of electronegative gas in a mixture in terms of the gas pressure P (in atmospheres), and Shubweg δ (in cm) based on gas-discharge theory:

$$C \approx \frac{7 \cdot 10^{-2}}{\delta P} \qquad \text{(III-3)}$$

The Shubweg δ is the product of the mean free life of the electron and its drift velocity under the applied field. Values representative of the case in many gases were assumed for the electron mobility and probability of attachment per collision, h, for the gas.

Suppose we wanted a gas purity that would make h' in our expression for relative variance equal 0.99. If an electron started a distance r from the central wire of a counter, the probability of its reaching the wire without attachment, by the definition of the Shubweg δ, would be $e^{-r/\delta}$. Therefore we set $e^{-r/\delta} = 0.99$ or $\delta \approx 100\ r$. For a counter in which 3 cm would be a representative value for r and at a pressure of 2.5 atoms we get, from Eq. (III-3), C = 0.01%, a fairly stringent requirement. If we try $h' = 0.9$ and make the same assumptions, we get $C \approx 0.1\%$, or 99.9% purity required. Now, going back to the approximate expression for relative variance and assuming $m_0 = 10^4$, we can solve for a value of h' that would give a relative variance of, say, 0.1%. This turns out to be a seemingly very easy criterion, $h' = 0.179$. However, making the same assumptions as before, we find C is about 1%. But in the equation for C the assumptions for electron mobility and h, which exhibits resonances for some gases dependent on electron energy, could both conceivably be off by almost a factor of ten, and considering also other approximations, we could easily be back to our 99.99% purity requirement. The parameters in the gas-discharge theory are not accurately known for all the pure gases and cannot be predicted for mixtures, especially if the percentages are not very accurately known.

RADIOACTIVE BACKGROUND

The problem is different if there is an appreciable tritium impurity in the helium-3 supply. The loss of energy resolution is then due to the pile-up of low-energy background counts due to the radioactive decay of the tritium. This decay has an end-point beta energy of about 18.9 kev [27].

To estimate the required purity of helium-3 with respect to tritium we must first analyze the effect of pile-up in general[21]. Consider the piling up of square pulses of uniform height W and equal width τ. A pulse height n W is produced if n pulses occur within a time τ. If a scaler discriminatpr level were set at n W, an erroneous count would then be registered. We can get approximate values for a counter by taking τ equal to the equipment resolving time.

If the occurrence rate of events in the counter each giving rise to an energy E has a mean rate of n_0, the mean number of events during a resolving time is $n_0\tau$ and the standard deviation is $\sqrt{n_0\tau}$ for $n_0\tau \gg 1$. Thus, the energy dissipated per resolving time is $n_0\tau\, E \pm \sqrt{n_0\tau E}$. Now suppose the threshold energy of the system is such that it takes an energy of $n\tau E$ to produce a spurious count. Then the following expression gives the number of standard deviations by which the number of counts during a resolution time must exceed the mean number in order for a spurious count to be produced:

$$(n\tau - n_0\tau)/\sqrt{n_0\tau} = [(n - n_0)/\sqrt{n_0}]\sqrt{\tau}. \qquad \text{(III-4)}$$

From this we can estimate the probability p_s of receiving a spurious count during the resolving time for a given n_0 and τ. The spurious counting rate is given by $I_s = p_s/\tau$. If we estimate τ as 0.5 μsec and wish to keep I_s less than 0.1 count per minute, p_s must be less than $I_s\tau = 5/6 \cdot 10^{-9}$. This probability corresponds to a deviation above the mean between 5 and 6 standard deviations. Let us require that n_0 be less than n by 6 standard deviations. The average energy of the tritium beta spectrum is about 5.7 kev, therefore let E equal this

value. The range of beta particles of this energy is such that most of the beta energy will be spent in the counter gas, as shown in Chapter VI. Since the Q of the He^3 (n, p) T reaction is 770 kev, a value of $n\tau E$ less than this will not be detected as a spurious count. Of course, a value of $n\tau E$ that is an appreciable fraction of 770 kev destroys the accuracy of neutron-energy determination if enough of the pile-ups occur in coincidence with valid neutron counts. However, the number of accidental coincidences between two counting rates is proportional to the product of the rates and the resolving time; in this case the true and spurious rates are expected to be small enough that the problem of modification of true pulse-height counts will not be as serious as the number of spurious counts recorded compared to the number of true counts. If we set $n\tau E = 770$ kev, n is approximately $3 \cdot 10^8$. Using Eq. (III-4), we obtain

$$6 = \left[\frac{3 \cdot 10^8 - n_0}{n_0^{1/2}}\right](0.5 \cdot 10^{-6})^{1/2} .$$

Solving, we have $n_0 = 1.86 \cdot 10^8$ disintegrations per second.

If this is the allowable mean disintegration rate, we can solve for the allowable number of tritium atoms in the counter from the disintegration equation:

$$dN/dt = -(0.693/T_{1/2})\,N = -n_0 ,$$

where

N = number of tritium atoms

$T_{1/2}$ = tritium half life = 12.26 years.

This gives $N = 1.03 \cdot 10^{17}$ tritium atoms. Or if each molecule is diatomic, the allowable number is $5.65 \cdot 10^{16}$ molecules. The sensitive volume of the central counter is $V_c = 888$ cc, and at P = 2.5 atmospheres, the total number of molecules is $D\,P\,V_c = 5.66 \cdot 10^{22}$ molecules, where D = Loschmidt's number at 15° C, or $2.55 \cdot 10^{19}$. This gives a tritium composition of about 0.0001%. This looks like a

very serious purification problem if there is significant tritium contamination in the helium-3 supply.

SATURATION EFFECTS

It is apparent that for high-energy particles and high enough multiplication, saturation effects near the wire should eventually destroy the proportionality of the multiplication process. Experimentally, the ratio of pulse sizes has been found accurate to 1.5% for M less than a critical value of $M_c(E)$ at which saturation effects begin[28]. For the counter used the experimenters found

$$E \cdot M_c(E) = \text{constant} = 10^8 \text{ ev.} \qquad \text{(III-5)}$$

Using this for our counter application, where the maximum $(E_n + Q)$ is 1.77 Mev, and allowing a safety margin of a factor of two, we have

$$M_c \ (E = 1.77 \text{ Mev}) \approx 28 .$$

If we also check expected charge-to-length ratio in avalanche compared to charge-to-length ratio on the wire, a ratio of 4% corresponding to Eq (III-5), it appears that adoption of the equation for this counter should ensure no significant loss of proportionality due to saturation. High values of multiplication are also not desired, owing to increased voltage-stability requirements, because the curve of multiplication versus counter voltage in most cases starts out rather flat but soon rises into a steep ascent.

POSITION OF IONIZATION

Because of the long travel time of positive ions to the cathode, amplifier time constants must be used that ignore part of their contribution to the pulse. This makes the size of the pulse dependent on the position of ionization. A general rule is to use $M > 10$ to avoid this effect when counter radius is 100 times wire radius. Let us investigate the effect for our counter, for $y = b/a = 1000$, and for no multiplication. On the basis of the expressions for fraction of total

induced voltage due to electrons and positive ions, Staub shows that the fraction of the volume of the chamber in which the ionization can originate so that more than half of the pulse is caused by the fast electron collection is b/(b+a), since the contribution to the pulse is evenly divided when $r = \sqrt{(a \cdot b)}$ is the position of original ionization[10]. Or this is y/(y+1), which equals 1000/1001, which seems to indicate that multiplication might not be necessary for large y values. This assumed position corresponds to r = 31.6a for our counter. As a further check we assumed the ionization took place at r = 316 a, and calculated the fraction of the pulse due to electron motion (ionization in about 90% of the volume would give larger pulses), using the assumptions about ionic motion used in Chapter II and some other equations from Reference 18. This fraction was 0.835. Amplifier time constants in reality would be long enough to register some of the positive-ion motion, which would improve this fraction. However, starting from r = 316a under the same conditions and assumptions, we calculate the ionic motion to contribute only about 0.002 to the total pulse in a collection time of 5 μsec. Thus we conclude some multiplication is necessary to remove effects due to position of ionization.

END EFFECTS

With no preventive measures there would be an abnormally high electric field at the ends of a counter wire. The loss in resolution thereby can be partially erased by having the wire shielded or thickened near the ends to give a low field. The variation of M along a counter wire has been measured and found to be important at a distance on the order of a counter radius from the thickened ends[29]. In a high-pressure proportional counter designed to be used for neutron spectroscopy it was found that the pulse-height distribution varied radically over the extent of the counter in a preliminary design without field tubes[12]. The loss of resolution compared with the resolution at the center, was significant when the

investigators moved a narrow pencil of thermal neutrons with which they were probing the counter 0.5 inch away from the center. The wire was about 8 inches long. The simplest way of overcoming end effects is to use a long counter--that is, long compared with the radius. Of course, this is not always practicable. Our counter, with wire length 21.6 cm and counter diameter 7.62 cm, is not a very long counter, and we might expect considerable loss of resolution due to end effects. The end effects can be eliminated by mechanical methods, which add complexity to the counter. A divided counter was constructed in which a bead divided the wire into two unequal lengths[30]. Subtracting one spectrum from the other eliminates end effects. Field tubes extending over a guard tube eliminate end effects when field-tube potential is adjusted to a proper value and field and guard tubes are correctly located. Field tubes were proposed in 1951[31] and used the same year[32] to investigate the low-energy spectrum of tritium down to approximately 200 ev.

WALL EFFECTS

Wall effects as outlined for a gas recoil chamber by Rossi and Staub[21] are pertinent for charged-particle reactions, since in both cases the loss in resolution results when the particle that causes the ionization in the gas does not expend its full range in the sensitive volume. Three cases are: (a) The reaction takes place in the sensitive volume but one of the charged particles produced crosses the end boundary; (b) The reaction takes place in the sensitive volume but the charged particle hits the lateral wall; (c) The reaction takes place outside the sensitive volume, but one of the charged particles enters the sensitive volume. The anticoincidence ring does not help in those instances in which the charged particle crosses the ends. Thus, it is desirable to have a small ratio of area of ends to lateral area, or--what is the same thing--a long counter, as in reducing end effect. Pulses reduced in size by the wall effect contribute a continuum of energies from zero to $(E_n + Q)$ to the

pulse-height distribution. Without the use of an anticoincidence ring or a magnetic field to curve the paths of the charged particles, the wall effect can be reduced only by increased size of the counter and increased gas pressure.

OTHER EFFECTS

Inaccuracies in energy resolution can also come from variation in applied voltage, variation in position and diameter of the wire, and dust particles on the wire. These are discussed in the general references. Any alone could be very detrimental, but it appears that all can be avoided with careful techniques.

CHAPTER IV

GAS FILLINGS

The counter was first tested by filling from a bottle of argon plus 4% carbon dioxide. The filling and evacuation system used had an oil diffusion pump and liquid nitrogen trap, but no special purification procedure or trap was used in the gas-filling line. Satisfactory operation was obtained in counting gamma rays at pressures of one, three, and five atmospheres. Since the secondary electrons have a continuous distribution of pulse heights, we would not expect a flat plateau in the curve of counting rate versus voltage in the proportional region, but we do desire a slope that does not place too exacting requirements on voltage regulation. At 5 atmos we found about $\frac{1}{2}$% increase in counting rate per volt in the 2600-to-2700-volt range on the main counter. This was at a high value of M; the range of pulse heights available was several thousand times the minimum detectable pulse height. At 3 atmos in the same voltage range, the change in counting rate per volt was about 3%. Of course, the M was greater owing to the lower pressure. The ring counter at 5 atmos had about 1% increase per volt in the 2100-to-2200-volt range. Its counting rate was higher owing to its proximity to the wall.

The helium filling was from a bottle of 99.99% pure helium; the desired percentage of carbon dioxide was previously introduced through a separate filling line. Both filling lines were run through dry ice–acetone slush traps when CO_2 was used or a liquid nitrogen trap if helium alone was used. (CO_2 would be frozen out by a liquid nitrogen trap.) The use of the traps did not seem to have a large effect. The CO_2 was found very necessary to avoid spurious discharges in the counter.

The stabilizing effect of polyatomic gases mixed with noble gases seems to depend on their ability to absorb photons, in contrast to the small-photon capture cross section of the noble gases (many of these photons are produced by metastable atoms), and also possibly on their

ability to receive energy from metastable states that have high excitation energies. Colli has investigated ultraviolet photons in the decay of metastable argon atoms and found them to be responsible, through a photocathodic process, for the starting and maintenance of corona current in cylindrical argon counters[33]. The photons were produced in the Townsend avalanche on the wire. Another effect of metastable atoms is the release of secondary electrons from metal surfaces[34]. The positive ions can also eject secondary electrons from metals, the requirement being that the energy of ionization be greater than twice the work function of the metal, which is about 5 ev for common cathode walls. Helium is expected to be more troublesome than other gases because of its high ionization potential, about 24.5 ev, and the high energies of its metastable atoms, about 20 ev. Evidence for the difficulty of interpreting experiments with helium has been presented[35] on the basis of the existence of the helium molecule-ion and metastable molecule. It had been shown the He_2^+ ion is present at very low pressures, and the concentration increases with pressure relative to the concentration of He^+.

The stabilizing effect of CO_2 was demonstrated in the counter by determining the approximate maximum voltage on the main counter that could be applied without causing a rapid breakdown when a radioactive source was placed a given distance from the counter. Total pressure was 5 atmos. The results are listed in Table II. The breakdown caused by background radiation alone occurs with pure helium at 800 volts.

However, adding more CO_2 was not a solution because the pulse heights were thereby drastically reduced. It had been found previously that in mixture of argon plus 10% CO_2 there was a loss of pulse height above pressures of 3 atmos, probably due to columnar recombination, which is high in CO_2. This refers to recombination along the track of a densely ionizing particle. It was not possible to attain a large enough range of pulse heights above a minimum discriminator setting for counting recoils from a Pu-Be (α, n) neutron

Table II. Percentage of CO_2 in helium versus voltage for breakdown on main counter.

Percentage of CO_2	Critical Voltage
4	1500
6	2000
12	2500
20	2800
25	3000
33-1/3	----

source without going to a counter voltage at which spurious discharges would occur. The situation improved with decreasing pressure.

A final filling at 2.5 atmos with 2% CO_2 was chosen for further experimentation. The curve of counting rate versus voltage for counting neutron recoils from the Pu-Be source showed a slope of 0.84% change in counting rate per volt in the range of 1100 to 1200 volts on the main counter wire. For the outer wire there was a 4.3% change in counting rate per volt in the range from 800 to 1000 volts. The voltage-stability requirements at 5 atmos at a voltage at which the spurious discharges did not occur were not significantly different.

One advantage of helium as the counting gas is readily apparent--its reduced sensitivity to background gamma radiation. The range of the secondary electrons in g/cm^2 is about the same, but helium has about 1/10 the density of argon. The low atomic number of helium is also an advantage in that the interaction of gamma rays directly with the gas is small.

CHAPTER V

COUNTING RATE AND EFFICIENCY

For an isotropic neutron flux in a proportional counter the counting rate may be expressed[2] as

$$I = N V_c \int \sigma(E_n)\ \phi_{E_n}\ F(E_n)\ \ f(E_n)\, dE_n ,$$

where

N = density of reacting nuclei (nuclei/cm^3),

V_c = volume of absorbing material (cm^3),

$\sigma(E_n)$ = neutron cross section of absorbing nuclei (cm^2),

ϕ_{E_n} = neutron flux per energy interval (neutrons/cm^2-sec-erg),

$F(E_n)$ = detection efficiency defined as ratio of counting rate to rate of reacting events.

Ideally, for an exoergic reaction and integral detection, $F(E_n)$ is a step function: zero for $E_n < B$ and unity for $E_n > B$, where B is threshold bias energy for equipment. This step function is modified by a geometric factor, $G(E_n)$, for wall effect as shown below. For differential detection, $F(E_n)$ is ideally a difference between two step functions with thresholds B_1 and B_2. For a recoil-detection process in which, with no collimation, a neutron of any energy may give pulses from zero to a maximum, we must evaluate $F(B/E_n)$, which gives the fractional number of recoils giving pulses larger than B. Thus, for a recoil detector, one has

$$F(E_n) = G(E_n)\ F(B/E_n).$$

The term $f(E_n)$ above is a correction factor for perturbation of flux caused by insertion of the absorber. This factor is neglected in the rest of the discussion.

A solution of the equation for counting rate would in most cases be extremely complicated. Some insight can be gained by considering the simpler case of a monoergic neutron flux. Then we can eliminate the differential and replace ϕ_{E_n} with $\phi\ (E_n)$ in neutrons/cm^2-sec.

For neutrons of a given energy this leads to

$$I = N V_c \sigma(E_n) \phi(E_n) F(E_n) .$$

The efficiency of a counter is defined as I/q, where q is the number of neutrons per second traversing the counter volume; $q = \phi(E_n)A$, where A is the effective exposed area of the counter. Then counter efficiency is

$$e_C = \frac{N V_c \sigma(E_n) \phi(E_n) F(E_n)}{\phi(E_n) A} = \frac{N V_c \sigma(E_n) \phi(E_n)}{A} .$$

If we call $V_c/A = d$, the average distance traveled by a neutron in crossing the counter[24], counter efficiency is

$$e_C = N \sigma (E_n) d F(E_n) = e_R F(E_n) ,$$

where $e_R = N \sigma (E_n) d$ is the efficiency of radiation defined as the ratio of the rate of reacting events to rate of neutrons traversing the counter volume.

The quantity N is readily calculated by expressing it as D P, where D is Loschmidt's Number and P is the pressure in atmos.

For the counter, we have d = 1.59 cm if we take the total surface area of the main counter as the effective exposed area for an isotropic flux. If we assume 2.5 atmos of helium-3 and a neutron energy for which the (n, p) cross section is one barn, we have $e_R \approx 0.01\%$. For the counter filled with ordinary helium at the same pressure and for a neutron energy for which the scattering cross section is 2 barns, we have $e_R \approx 0.02\%$ for recoils.

The opposite extreme to an isotropic flux is a collimated neutron beam. Here the general equation for counting rate is

$$I = A \int \phi_{E_n} (1 - e^{-N \sigma(E_n) T}) F(E_n) dE_n ,$$

where

A = area perpendicular to beam,

T = thickness in cm of material parallel to beam.

Assuming a monoergic neutron beam as before, we can write

$$I = A\,\phi(E_n)\,[1 - e^{-N\sigma(E_n)T}]\;F(E_n),$$

$$e_C = [1 - e^{-N\sigma(E_n)T}]\;F(E_n) = e_R\,F(E_n),$$

and for $N\sigma(E_n)T \ll 1$, $e_R \approx N\sigma(E_n)T$.

In this case we see that the radiation efficiency of a cylindrical counter in a neutron beam is dependent on its orientation with respect to the beam. If the beam direction is perpendicular to the long axis of a counter of radius b, solving for the average thickness of path gives $(\pi/2)b$ or 5.98 cm for the main counter. Thus, the counter has a higher radiation efficiency under these conditions by the factor $T/d = 3.76$. Of course, e_R would be even higher for a beam down the long axis of a cylindrical counter.

EXPERIMENTAL SETUP

However, in experimental setups the counter usually is neither in an isotropic flux nor exactly in a beam. Consider placing a neutron source at point P, a distance c from the counter axis and opposite the center of its length, as shown in Fig. 4. If c is not too small and the counter dimensions not too large, it seems we could approximate the expected counting rate by assigning an average neutron flux to the counting volume:

$$\phi_{av} = Q_s/4\pi r^2_{eff},$$

where Q_s = rate of emission of neutrons by the source and $r_{eff} = \sqrt{(c\,d)}$, where $d = \sqrt{b^2 + f^2 + c^2}$. Then,

$$I = N\,V_c\,\sigma\,Q/\,4\pi c\,d$$

(assuming $F(E_n) = 1$ for the time being). The rate for neutrons traversing the counter in neutrons per second can then be expressed as this average flux times the area of the central rectangle, or

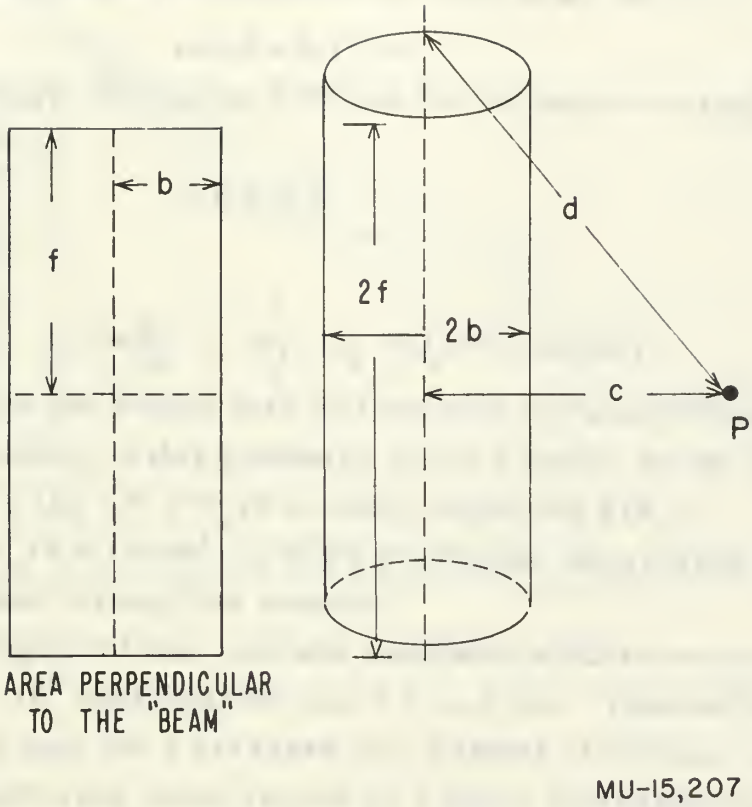

Fig. 4. Geometrical arrangement of neutron source and counter.

$$q = \frac{Q_s}{4\pi cd} \cdot 2b \cdot 2f = \frac{Q_s}{\pi} \cdot \frac{bf}{cd} \quad .$$

This expression was set down to show that this method is equivalent to a common method of computing the solid angle subtended by a finite rectangular counter[18]. For one of the small rectangles of area b f in the geometry shown the equation for solid angle given is

$$\tan \Omega = b\, f/c\, d$$

For a small angle we have $\tan \Omega \approx \Omega$ and for the entire rectangle the solid angle would be

$$4\, b\, f/c\, d.$$

Thus, we have

$$q = \left(4\frac{bf}{cd} \;/\; 4\pi\right) \cdot Q_s = (Q_s/\pi) \cdot (bf/cd)\,,$$

as above. Also one should note that we have assigned the same radiation efficiency in this geometry as for a beam, as we can show

$$e_R = I/q = N \sigma V_c/4\, bf \text{ (still neglecting } F(E_n)).$$

But we have $V_c/4\, b\, f = \pi b^2 \cdot 2\, f/4\, b\, f = (\pi/2)b$, the average thickness found for a beam through the counter.

An arrangement like this was used with a Pu-Be neutron source of $Q_s = 1.54 \cdot 10^6$ neutrons/sec and d = 21.2 cm. Then we compute $I/F(E_n) = 1662$ cpm for a pressure of 2.5 atmos of helium, and using an average scattering cross section of 2 barns corresponding to an average neutron energy of about 4 Mev. (Actually the Pu-Be neutron spectrum is complex from zero to about 11 Mev, and no attempt has been made to compute an accurate average value.)

If we obtain curves at different values of high voltage, as shown in Fig. 5, we can estimate the point where they tend to zero pulse height. At this point $F(E_n)$ is unity and the experimental value of counting rate should correspond to 1662 cpm. It appears to be only about 400 cpm, not a close correspondence, but there were so many inexactly known quantities and dubious averaging processes that it is

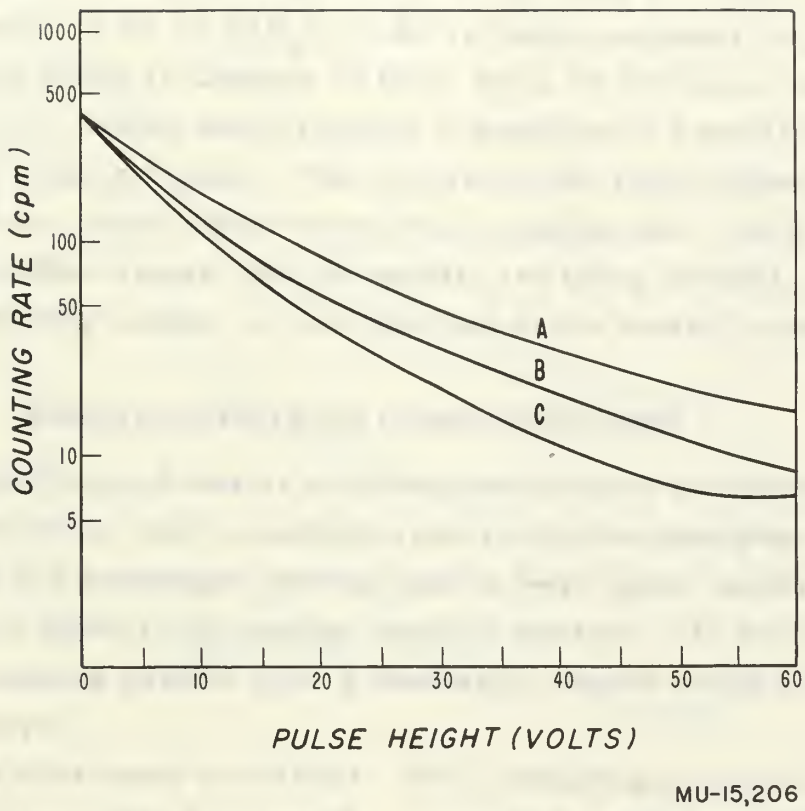

Fig. 5. Integral bias curves for main counter at various counter voltages,
A. 1200 volts,
B. 1165 volts,
C. 1135 volts,
and using neutron source in arrangement of Fig. 4.

hard to draw definite conclusions. The scattering cross section is rapidly varying in this energy range and the manner in which the integral bias curve approaches zero is not known. Also consider the counting rate of 175 cpm for the highest counter voltage used at a pulse height of 10 volts, the lowest discriminator setting for which counts were recorded. If we let $G(E_n) = 0.83$--a value computed for an average alpha recoil in Chapter VI then, for a 10-volt bias, we have $F(B/E_n) = 0.127$, which would indicate a detection of a small fraction of the recoil alpha particles. The curves for the ring counter, Fig. 6, seem to tend to a much higher zero-point counting rate, but it is believed that other events than the recoils are being counted, since the volume of the ring counter is less than that of the central counter.

RECOIL-SPECTRUM CONSIDERATIONS

It should be much easier to draw some definite conclusions about the suitability of the tube's multiplication factor for obtaining usable pulse heights if a monoergic neutron source were used, preferably one giving a recoil alpha in the energy range of interest, 770 kev to 1.80 Mev. The counting results from a monoergic source would be much easier to analyze.

This is illustrated as follows. For a monoergic source the neutron spectrum, $N(E_n)$ versus E_n, is ideally a spike and $N(E_n)$ is the total number of neutrons; the differential pulse-height spectrum due to the recoils, $n(W)$ versus W, where W is pulse height, is a rectangle; and the integral bias recoil spectrum, $N(W)$ versus W, is ideally a constant-slope line. These are sketched in Fig. 7. These shapes of the differential and integral bias curves are justified as follows. The pulse height depends on the energy of the recoil nucleus; the counter and amplifier convert that energy into pulse height. The recoil nucleus, as shown in Chapter VIII, can have a maximum energy of $K_a E_n$, where $K_a = 4A/(1 + A)^2$, if we use mass numbers for the masses. Let W be the energy of recoil nucleus (converted into volts of pulse height by the counter system). Then W can vary from 0 to

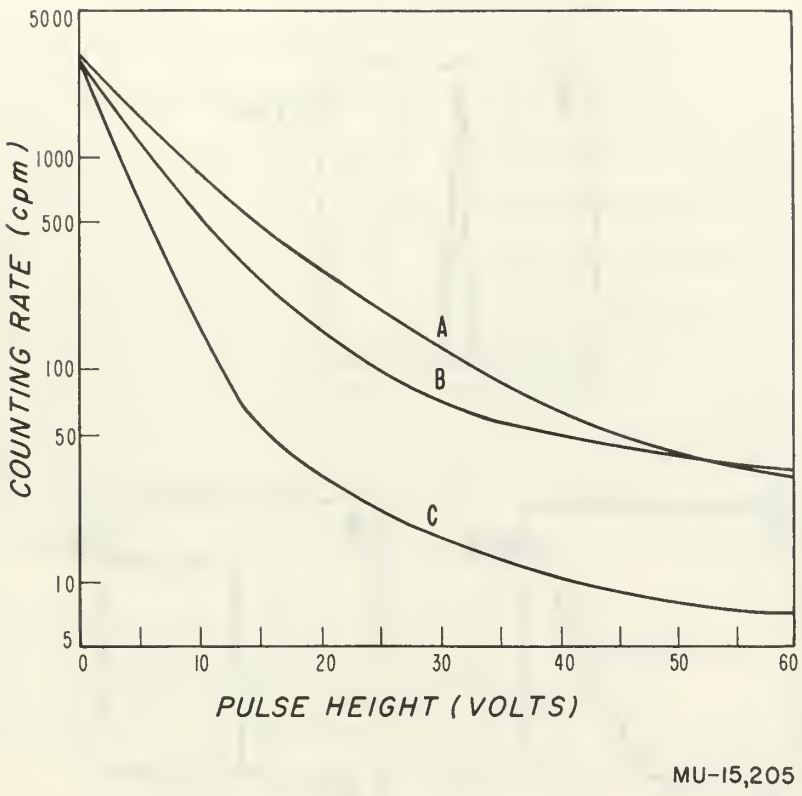

Fig. 6. Integral bias curves for ring counter at various counter voltages,

A. 1025 volts,
B. 975 volts,
C. 925 volts,

and using neutron source in arrangement of Fig. 4.

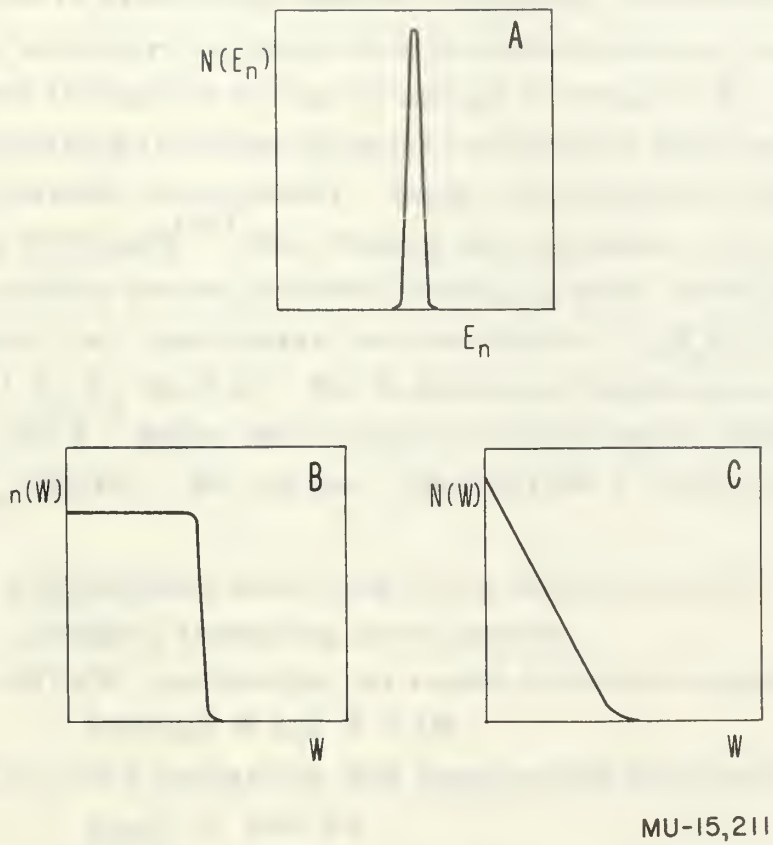

Fig. 7. Ideal curves for monoenergetic neutron spectrum.
A. Neutron spectrum.
B. Differential bias recoil spectrum.
C. Integral bias recoil spectrum.

$K_a E_n$ and the number of pulse heights from recoils from the monoergic source are spread out over this range of W values. The question is whether or not the distribution is uniform over the range, giving a rectangle. At the values of E_n of interest here, and for light nuclei, it is accurate to assume that neutron scattering is mainly S-wave and spherically symmetric in the center-of-mass system of coordinates. We wish then to express the recoil energy in terms of E_n and the angle of scattering in center-of-mass coordinates (both energies in laboratory-system coordinates). Using conservation of energy and an equation developed[36] for relating the velocities of the neutrons in lab coordinates before and after scattering with θ, the angle of scattering in c.m. coordinates, we can show $W = \frac{1}{2} K_a E_n (1-\cos\theta)$; then $dW = \frac{1}{2} K_a E_n \sin\theta\, d\theta$. But in spherical coordinates, we have $d\theta = d\Omega/2\pi \sin\theta$, where $d\Omega$ = element of solid angle, therefore $dW = K_a E_n (d\Omega/4\pi)$. We can say $\text{Prob}(W)\, dW = (\sigma(\theta)/\sigma_s)\, d\Omega$, where

$\sigma(\theta)$ = differential scattering cross section (c.m.),

σ_s = integral scattering cross section,

$\text{Prob}(W)\, dW$ = probability for recoil nucleus to acquire an energy between W and W + dW,

$(\sigma(\theta)/\sigma_s) d\Omega$ = probability that neutron will be scattered through angle θ into $d\Omega$.

It follows: $\text{Prob}(W) = \sigma(\theta)/\sigma_s \cdot 4\pi/K_a E_n$. For an isotropic scattering distribution ($\sigma(\theta)/\sigma_s = 1/4\pi$) and monoergic neutrons, Prob(W) is thus a constant, $1/K_a E_n$, and n(W) is a rectangle of constant value proportional to $N(E_n)$. The integral bias distribution is an integral of the rectangle, integrating from maximum W to zero, giving the triangular shape.

For a non-monoergic neutron spectrum, $N(E_n)$--instead of being the total number of neutrons--represents the number of neutrons per energy interval, and we must integrate over the spectrum. We can say

$$n(W) = K_1 \int \text{Prob}\,(W)\, N(E_n)\, \sigma_s(E_n)\, dE_n = K_1 \int 1/K_a E_n \quad N(E_n)\, \sigma_s(E_n) dE_n$$

where K_1 is an arbitrary constant and $\sigma_s(E_n)$ is the elastic scattering cross section as a function of neutron energy. Thus for a complex neutron spectrum the shapes of the differential and integral bias curves are very difficult to predict. For performing the integration in analytical form an expression for $N(E_n)$ and $\sigma_s(E_n)$ must be used. Generally, for most sources $N(E_n)$ goes from zero at $E_n = 0$ to a maximum and back to zero at $E_n = E_n(\max)$. The intervening structure may be quite complicated. Let us assume $\sigma_s(E_n)$ varies as $1/\sqrt{E_n}$. This is approximately true[18] for scattering on protons for E_n between 0.2 and 5 Mev, an approximate relation being $(\sigma_s)_p \approx 4.5/\sqrt{E_n}$ for E_n in Mev and σ_s in barns. It is less true for helium, which has a peak of about 6.6 barns at 1.15 Mev and then tails off. Then if, for illustrative purposes, we assume

$$N(E_n) = E_n^{3/2} \sin E_n$$

where E_n goes from zero to $E_n(\max) = \pi$ in arbitrary units, we have a spectrum shape that can be readily integrated:

$$n(W) = K_1 \int_{E_n = W/K_a}^{E_n = \pi} 1/(K_a E_n)\; E_n^{3/2} \sin E_n\, E_n^{-1/2}\, dE_n$$

$$= \frac{K_1}{K_a}\,(1 + \cos (W/K_a)),$$

where W goes from 0 to $K_a \pi$. To save writing W/K_a as the variable on the next integration, let us change W from energy to arbitrary voltage units where W goes from 0 to π. Since we have divided the W scale by K_a, we must multiply the density distribution by K_a. The differential distribution becomes

$$n(W) = K_1 (1 + \cos W).$$

The integral bias distribution is obtained by integrating this from the right:

$$N(W) = -K_1 \int_{\pi}^{W} (1 + \cos W)\, dW = K_1 (\pi - W - \sin W).$$

The value of this distribution at $W = 0$ is the total number of scattering events, πK_1. This should equal the number of neutrons times the probability of scattering or

$$K_1 \int_0^{\pi} N(E_n)\, \sigma_s(E_n)\, dE_n = K_1 \int_0^{\pi} E_n \sin E_n\, dE_n = \pi K_1.$$

The three distributions are sketched in Fig. 8. The significant trend is the way the integral bias distribution rises rapidly near zero pulse height, even with this assumed neutron spectrum weighted heavily toward the high-energy end of the spectrum. With a complex neutron-energy spectrum--as obtained, for example, from (α, n) sources [37]--the shape of the integral bias curve and the manner in which it tends to the zero pulse-height counting rate becomes very difficult to predict.

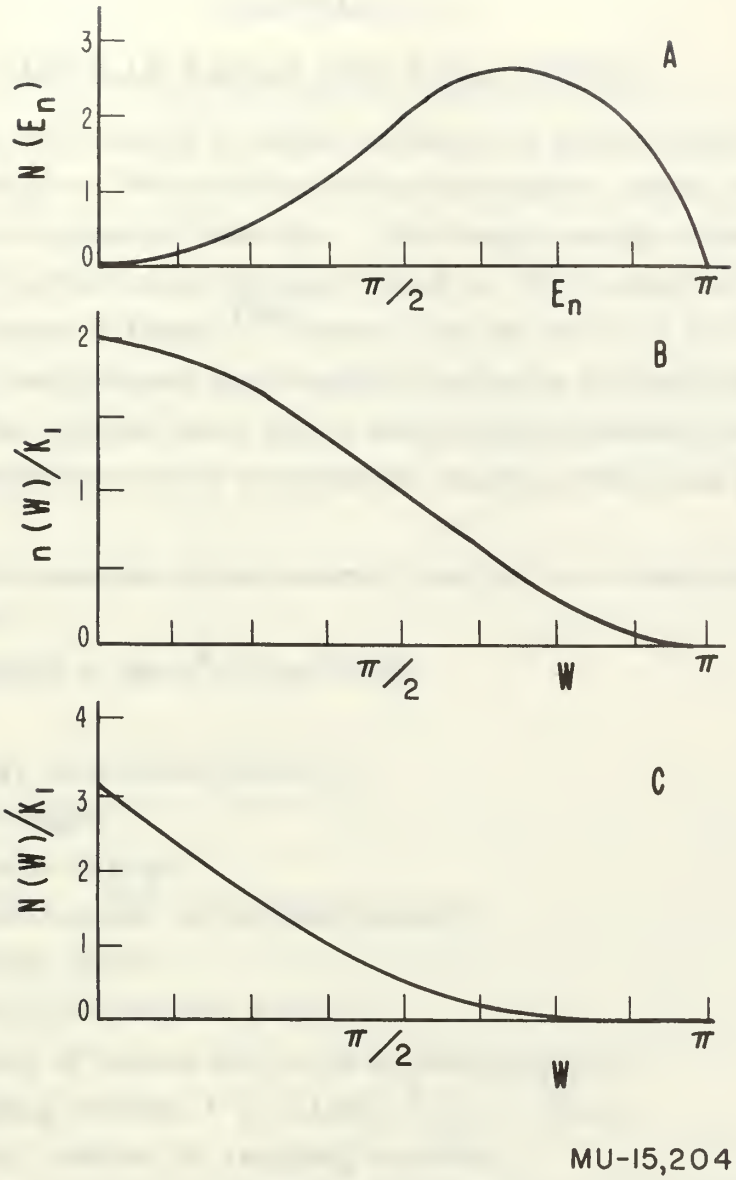

Fig. 8. Assumed neutron spectrum and recoil spectrum for assumed conditions.

A. Neutron spectrum.
B. Differential bias recoil spectrum.
C. Integral bias recoil spectrum.

CHAPTER VI

PARTICLE RANGE AND WALL EFFECT

Knowing the range of an alpha particle or proton in air, we can compute the range in helium if we know the relative atomic stopping power of helium compared with air. The range-energy curves to be used for alpha particles and protons in air at 15° C and 760 mm pressure are those of Bethe,[38] which, on the basis of experiment, corrected for low energies the original curves by Livingston and Bethe[39]. The original work was a theoretical treatment based on the Born approximation but also modified by experimental data then available.

The basic equation giving energy loss per cm of path defines stopping power:

$$- dE/dR = (4\pi e^4 z^2/mv^2) NB,$$

where

E = energy of incident particle,

R = path length,

e = electron charge,

z = atomic number of incident particle,

m = electron mass,

v = velocity of incident particle,

N = number of atoms per cc of stopping material,

B = stopping number = $Z \ln (2m v^2/I_{av})$, where

Z = atomic number of stopping material,

$I_{av} = K Z$ = average excitation potential of atom of stopping material,

K = Bloch constant (which is not actually a constant but varies somewhat for different atoms and is usually determined experimentally because it is difficult to calculate theoretically).

The relative stopping power, compared with air, is defined:

$$s = B/B_0 = Z/Z_0[(\ln 2mv^2 - \ln I_{av})/(\ln 2mv^2 - \ln I_0)] ,$$

where the zero subscripts refer to air. Here s is seen to be a function of incident-particle velocity, and for different atoms increases more slowly than Z alone. We find it accurate enough for the purpose at hand to use this equation, although many modifications to the theory can be made in computing B, as done by Hirschfelder and Magee[40] for several different substances for protons.

We take experimentally determined values of air from Reference 39: $I_0 = 80.5$ ev and $Z_0 = 7.22$. For helium, $I_{av} = 44$ ev[41]. The calculation shows, for 1-Mev protons, $s_{He} = 0.328$. To convert the range in cm in air at NTP (15° C, 760 mm) to that in helium under the same conditions we note that stopping power is proportional to N and B, therefore the range in cm must be inversely proportional to these quantities. The range in helium is

$$R = R_0 \cdot N_0/N \cdot s_0/s_{He} ,$$

where the zero subscripts again refer to air and $s_0 = 1$. Now, N_0/N is approximately 2, since air is mostly diatomic. The calculation yields $R = 6.13\ R_0$. This should be fairly accurate for helium-3 or helium-4. For a 1-Mev proton, R_0 is 2.28 cm, therefore R is 14.0 cm. The range is inversely proportional to gas pressure, since density is proportional to pressure. Thus, at 2.5 atmos this proton range in helium becomes 5.60 cm, and at 5 atmos, 2.80 cm.

To find the range of an ion of other isotopes of hydrogen (given the relation for protons) we note that of all terms in the stopping power formula only v^2 is different for a given energy. Thus, a triton of energy E experiences the same stopping power as a proton of energy 1/3 E; but it goes three times as far since it has three times the energy. The maximum triton energy with which we will be concerned in the He^3 disintegration is about 1 Mev, and we figure its range to be 8.54 cm in 1 atmos of helium. Since this is less than a representative proton range from a He^3 disintegration and represents an upper bound on the triton range, the order of magnitude of the

wall-effect difficulties can best be estimated by considering the proton range. As pointed out by Batchelor[7] in explaining his computer program for wall-effect computation, the correlation between proton and triton tracks plus a cylindrical geometry makes exact calculations impracticable; also the angular distribution of the $He^3(n, p)T$ reaction is not very well known.

In integral bias counting involving the (n, p) reaction, detection efficiency is defined as the counting rate divided by rate of emission of protons. When the total range of particles is small compared with linear dimensions of a counter and distribution is isotropic, a value for detection efficiency often given is

$$F(E) = 1 - R_E/2\,b - R_E/2\,L,$$

where we have an active cylindrical volume of radius b and length L, and R_E is that portion of total range of protons necessary to produce a pulse above the bias energy E of the discriminator[10]. The terms in the expression for F(E) reducing it from unity represent the magnitude of the wall effect and indicate the loss at the lateral boundary and end face, respectively.

The expression for F(E) can be shown to be plausible as follows: Consider the fraction of the volume of a cylinder of radius b within a distance R of the side walls. This fraction is $(2\,bR - R^2)/b^2$. Consider charged particles originating with equal probability along a radial line with ends defined by the outer volume. If any direction of emission is equally probable, one-half of the particles will be emitted with a radial component toward the center and not intercept the wall. For that half of the particles having a positive radial component, those originating on the inner edge of the fractional volume have practically zero probability of intercepting the walls (since only one direction of emission allows the particles to reach the wall), while those originating at the wall have 100% probability of reaching the wall. Assuming that this increase in probability is linear as we move outward toward the wall, we estimate that one-fourth of all the particles

originating in the fractional volume reach the wall. Then the wall effect is 1/4 time the fraction of the volume, or

$$R/2b - (R/2b)^2 .$$

For $R \ll 2b$, this is approximately $R/2b$. Similarly, the fractional volume within a distance R of the ends of a cylinder is $2R/L$, and--again taking 1/4 of this value--we get $R/2L$ as the wall effect due to the ends.

In our case the condition of large dimensions is not well fulfilled; also we assumed that the ionization from the particle other than a proton was confined to a very small region, which is not so true for a He^3 reaction as for one involving heavier nuclei. In differential detection F(E) is ideally the difference between two step functions with different energy thresholds. Therefore, the deviation from unity is a rough indication of the magnitude of wall effect on energy determination for a proton of given energy. For a 1-Mev proton in 2.5 atmos of helium, the geometric factor is

$$G(E=1 \text{ Mev}) = 1 - R/2b - R/2L,$$

and with $2b = 7.62$ cm, $2L = 38.9$ cm, $R = 5.60$ cm, we have $G(E)=0.12$ or the wall effect is 88%. Doubling the pressure would reduce the wall effect to 44%, and at 10 atmospheres to 22%.

For counting neutrons in ordinary helium we are concerned with the range of the alpha recoil. The maximum energy of the alpha particle is $16/25\ E_n$, as shown in Chapter VIII. If we consider the average energy of the Pu-Be neutron spectrum to be 4 Mev, this corresponds to a maximum alpha energy of 2.56 Mev, or an average E_α of about half this amount. Figuring the range of this alpha particle in 2.5 atmospheres of helium by our previous method, we get 1.38 cm. The wall effect is 22% for this range. Experimentally, a coincidence counting rate of about 16% of the total counting rate in the main counter was measured. This is a very rough check, but it at least appears that the ring counter is capable of reducing the wall effect.

ELECTRON RANGE

To obtain the range and energy loss of electrons in estimating the effect of tritium decays or background gamma counts, one can take the nearest tabulated value[41] of stopping power for helium as a function of electron energy, given in units of Mev per g/cm^2. For example, at 10 kev, we have

$$- dE/dx = 22.5 \text{ Mev}/g/cm^2 .$$

If we take Δx as the average path in the counter, 1.59 cm, times the density of helium at 2.5 atmospheres, $\Delta x = 7.53 \cdot 10^{-4}$ g/cm^2. Then ΔE is greater than 16.9 kev (the product of $- dE/dx \cdot \Delta x$), because the stopping power increases with decreasing energy. For higher-energy electrons it is fairly accurate to use Feather's Rule or Flammersfeld's formula[20] to find x and then multiply $\Delta x/x$ times the energy of the electron.

CHAPTER VII

NEUTRON GENERATOR

For testing purposes one desires a monoenergetic neutron source. The complex spectrum of (α, n) sources has been mentioned; the other class of neutron sources using radioactive nuclei are the photoneutron or (γ, n) sources. These use deuterium or beryllium because other nuclei have thresholds above 6 Mev. To get high enough intensity the gamma source is surrounded so that there is an intrinsic energy spread due to different angles between neutron emission and incident gamma ray. This is small; for example, it is 3.37% for a $Na^{24} + Be^{9}$ source[20]. However, this is not the main cause of energy spread. Owing to the large quantity of beryllium there is considerable neutron scattering in the source, and gamma-ray loss of energy by Compton scattering.

It has been found possible to construct neutron generators utilizing the deuteron-deuteron reaction, $D(d, n)He^{3}$, with useful neutron intensities without elaborate high-voltage equipment; for example, the generator of Zinn and Seely[42] was built in 1937. Voltages on the order of 100 kv can give useful yields even though the reaction is not very efficient at this energy. With this low voltage we also have the advantage of almost monoenergetic and gamma-free neutrons. For a thick target the deuteron energy at the time of the reaction can vary from a maximum to zero. In the generator used in this experiment the maximum deuteron energy is 120 kev. Thus, using equations developed in Chapter VIII and $Q = 3.28$ Mev, we find that in the forward direction the neutron energy can vary from 2.46 to 2.91 Mev. At a laboratory-system angle of 90 degrees the energy spread is from 2.46 to 2.49 Mev, or little more than 1%. The energies are weighted toward higher values because yield increases rapidly with deuteron energy. This neutron-energy range is convenient for checking the operation of the counter because the maximum recoil-alpha energy is about the same as the maximum $(E_n + Q)$ energy we

wish to measure in helium-3, and about half the recoils are above the lowest sensitivity needed.

PULSED-NEUTRON GENERATOR

The neutron generator that is being put into operation provides a pulsed source of neutrons and is similar to the one described by Ruby[43] except for the method of mounting the accelerater system and the vacuum equipment. The accelerator system is described in Reference 43; briefly, the deuterons are generated in a pulsed Phillips Ion Gauge type of ion source supplied with deuterium gas through a palladium leak and accelerated to impinge upon a circular target of 1-1/8-inch diameter. The targets are prepared by occluding deuterium in titanium. This type of target allows simpler equipment than one with heavy ice, by requiring no special cooling. It is planned to try a deuterated paraffin target to see if the yield is increased. The objection of non-monoenergetic neutrons due to the $C^{12}(d, n)N^{13}$ reaction is not pertinent here because we are below the reaction threshold. The generator was designed so that adjustment of parameters would not be critical; the yield is largely determined by the accelerating voltage and the condition of the target. (The reaction cross section decreases with deuteron energy, and the targets have a tendency to form a carbonous surface after a few hours' use.)

The pulsed operation is particularly convenient for experiments that require a reference time, such as in neutron-diffusion experiments; single pulsing has been used for cloud chamber experiments. In normal operation the ion source is pulsed at 60 cycles per second with 200-μsec pulses. In this manner we can get an integrated yield, Q_s, of more than 10^6 neutrons per sec. This is a duty cycle of 0.012, or during a pulse the instantaneous neutron yield is $Q_s/0.012$ neutrons per second. For a cloud chamber experiment we used an external oscillator option of 400 cycles per second and increased the width of the pulse by an adjustment in the arc pulser to 500 μsec. This is a duty cycle of 0.2. This mode of operation was gated on, when it was

desired to take a picture, for 100 milliseconds, giving a total pulse-on time of 20 msec per gate. Then the neutron yield per gate should be $Q_s/0.012$ times 20 msec, or more than 10^6 neutrons in each burst, assuming the same effectiveness of the ion source when pulsed at 400 cycles per sec. as at 60 cycles. It would be more realistic to calibrate at 400-cycles steady operation, but this increases the risk of damage to the ion source.

NEUTRON YIELD

In order to measure the integrated yield one should determine if the anisotropy of the yield is significant. It has been found that in the energy region below 0.5 Mev, the neutron yield as a function of angle in center-of-mass coordinates can be represented[44] by

$$N(\theta) = A\ (1 + B \cos^2 \theta),$$

where A is a constant and B is a number that increases with deuteron energy. Thus, the yield is smallest at $\theta = 90$ degrees. The quantity B has been determined experimentally[45] down to 500 kev, and the curve extrapolates fairly well into a theoretical determination[46] at low energies based on the $D(d, p) H^3$ reaction. It is believed the angular asymmetry is the same for the companion reactions at corresponding voltages. We estimate B as 0.6 at 120 kev. This means the neutron flux at $\theta = 0$ should be (1 + B) times the neutron flux at $\theta = 90$ degrees. Or, performing an integration, we find that if Q_s is determined by measurements at $\theta = 0$, we should divide this by $(1 + (B/2+B))$ for the true yield or 1.23 for $B = 0.6$. This is a high estimate of the anisotropy, because not all the deuterons have the maximum energy. With these small deuteron energies, we expect that the laboratory-system angles will not be much different from the center-of-mass angles. We need not outline the calculations here (a description of the two coordinate systems and some convenient equations may be found in Reference 47), but for $\theta = 90$ degrees, we find the lab angle $\theta_L = 85.6$ degrees for 120 kev, and for $\theta_L = 90$ degrees, $\theta = 94.4$ degrees.

The generator yield has been monitored with a BF_3 proportional counter surrounded by 2.5 inches of lucite moderator and a thin sheet of cadmium. Care must be taken in its calibration since this arrangement does not give equal sensitivity over a wide range of neutron energies. For a particular counter we found a sensitivity of 0.29 counts per neutron per cm^2 when a Pu-Be source was used, and 0.37 counts per neutron per cm^2 when a mock fission source with a smaller energy range of neutrons was used. However, it can be calibrated on the D-d neutrons by comparison with a calibrated Hanson and McKibben type[48] long counter. The lucite embedded counter is easier to place and adds less scattering objects to the experimental arrangement.

CHAPTER VIII

NUCLEAR REACTION DYNAMICS

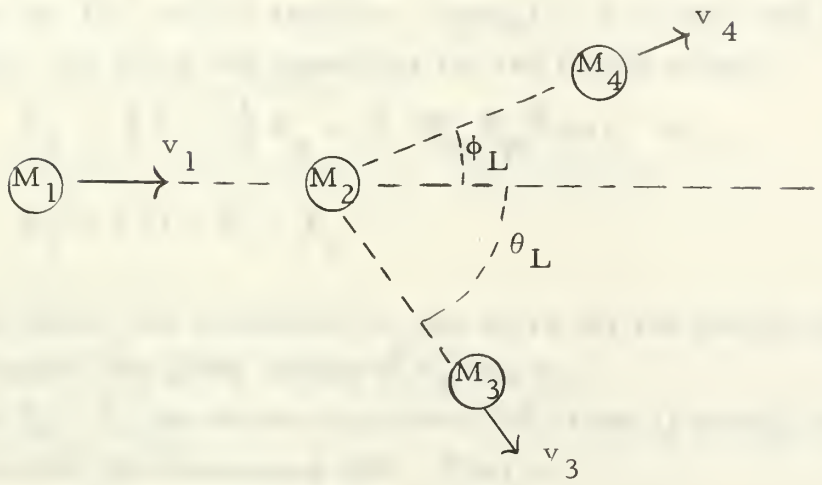

Consider the general case sketched above of a particle of mass M_1 and velocity v_1 colliding with a target nucleus of mass M_2 assumed at rest. After the reaction the resulting particle of mass M_3 flies off with velocity v_3 at angle θ_L. The nucleus of mass M_4 has velocity v_4 at angle ϕ_L. We will use nonrelativistic dynamics, mass numbers for masses, and laboratory coordinates.

First, write two equations for conservation of momentum for components parallel and perpendicular to v_1:

$$M_1 v_1 = M_4 v_4 \cos \phi_L + M_3 v_3 \cos \theta_L, \qquad \text{(VIII-1)}$$

$$M_3 v_3 \sin \theta_L = M_4 v_4 \sin \phi_L . \qquad \text{(VIII-2)}$$

By transposing the last term of Eq. (1) to the other side, squaring both equations and adding, we can eliminate ϕ_L. Then replacing velocities by use of $E = \frac{1}{2} M v^2$ for energy and rearranging, we obtain

$$E_4 = \frac{M_1}{M_4} E_1 + \frac{M_2}{M_4} E_3 - \frac{2}{M_4} (E_1 E_3 M_1 M_3)^{\frac{1}{2}} \cos \theta_L .$$

We can write another equation for E_4 from the definition of the Q of the reaction. Having assumed $E_2 = 0$, we write

$$E_4 = Q + E_1 - E_3 .$$

For the He^3 (n, p)T reaction, using Q = 0.77 Mev and similar symbolism, we write two equations for the triton energy:

$$E_T = \frac{1}{3} E_n + \frac{1}{3} E_p - \frac{2}{3} (E_n E_p)^{\frac{1}{2}} \cos \theta_L ,$$

$$E_T = 0.77 + E_n - E_p .$$

With these two equations we can solve for the proton and triton energies for given values of E_n and θ_L.

For $E_n = 0$, the proton receives 75% of the Q energy and the triton receives the remaining 25%. That is,

$$E_p = 0.577 \text{ Mev},$$
$$E_T = 0.193 \text{ Mev} .$$

For $E_n = 1$ Mev, a tabulation is given below.

θ_L (degrees)	Proton		Triton	
	E_p (Mev)	% of $(E_n + Q)$	E_T (Mev)	% of $(E_n + Q)$
0	1.74	98.3	0.03	1.7
45	1.52	85.8	0.25	14.2
90	1.08	61.0	0.69	39.0
135	0.77	43.5	1.00	56.5
180	0.67	37.8	1.10	62.2

It is often desirable to have a convenient expression for the energy of the ejected particle at $\theta_L = 0$ and at 90 degrees as a function of the bombarding particle energy. For the forward direction the two equations become

$$E_4 = \frac{M_1}{M_4} E_1 + \frac{M_3}{M_4} E_3 - \frac{2}{M_4} (E_1 E_3 M_1 M_3)^{\frac{1}{2}} ,$$

$$E_4 = Q + E_1 - E_3 .$$

A solution for E_3 yields

$$E_3 = A_2/2A_3 + \tfrac{1}{2} [(A_2/A_3)^2 - (4A_1^2/A_3)]^{\frac{1}{2}} ,$$

where

$$A_1 = M_4 Q + E_1 (M_4 - M_1) ,$$

$$A_2 = 2A_1 (M_3 + M_4) + 4 E_1 M_1 M_3 ,$$

$$A_3 = (M_3 + M_4)^2 .$$

For the He^3 (n, p) T reaction this gives

$$E_p = \frac{3}{4} Q + \frac{5}{8} E_n (1 + \frac{1}{5} [9 + \frac{12 Q}{E_n}]^{\frac{1}{2}}) .$$

For the D(d, n) He^3 reaction,

$$E_n = \frac{3}{4} Q + \frac{1}{2} E_d (1 + \frac{1}{2} [3 + \frac{6Q}{E_d}]^{\frac{1}{2}}) .$$

For θ_L = 90 degrees, the two equations are

$$E_4 = \frac{M_1}{M_4} E_1 + \frac{M_3}{M_4} E_3 ,$$

$$E_4 = Q + E_1 - E_3 .$$

Solving, we obtain

$$E_3 = \left[M_4/(M_3 + M_4)\right] Q + [(M_4 - M_1)/(M_4 + M_3)] E_1 .$$

For the two reactions above, at 90 degrees,

$$E_p = \frac{3}{4} Q + \frac{1}{2} E_n ,$$

$$E_n = \frac{3}{4} Q + \frac{1}{4} E_d .$$

For the case of elastic scattering we set $Q = 0$ and $M_3 = M_1$, therefore the two equations become

$$E_4 = \frac{M_1}{M_4} E_1 + \frac{M_1}{M_4} E_3 - \frac{2}{M_4} (E_1 E_3 M_1^2)^{\frac{1}{2}} \cos \theta_L ,$$

$$E_4 = E_1 - E_3 .$$

We are interested in the energy given to the recoil nucleus, therefore we eliminate E_3 from the first equation by using the second. Then we set $\theta_L = 180$ degrees for maximum E_4 corresponding to a backward recoil. Solving for E_4(max), we have

$$E_4 \text{ (max)} = \frac{4M_1M_4}{(M_1+M_4)^2} E_1 ;$$

For neutron scattering in helium-3,

$$E_{He^3} \text{ (max)} = \frac{3}{4} E_n ;$$

and for neutron scattering in helium-4,

$$E_\alpha \text{ (max)} = \frac{16}{25} E_n .$$

BIBLIOGRAPHY

1. P. I. Dee, Proc. Roy. Soc. (London) A136, 727 (1932).
2. B. T. Feld and P. Morrison, in Experimental Nuclear Physics, E. Segrè, Ed., Vol. 2 (Wiley, New York, 1953), Part 7.
3. B. J. Moyer, Nucleonics 10, No. 4, 14 (April, 1952); No. 5, 14 (May 1952).
4. B. T. Feld, Phys. Rev. 70, 429 (1946).
5. J. H. Coon, Phys. Rev. 80, 488 (1950).
6. D. J. Hughes and J. A. Harvey, "Neutron Cross Sections," BNL-325, July 1955.
7. R. Batchelor, R. Aves, and T. H. R. Skyrme, Rev. Sci. Instr. 26, 1037 (1955).
8. R. Wilson, L. Beghian, C. H. Collie, H. Halban, and G. R. Bishop, Rev. Sci. Instr. 21, 699 (1950).
9. A. Sayres and C. S. Wu, Rev. Sci. Instr. 28, 758 (1957).
10. H. H. Staub, in Experimental Nuclear Physics, E. Segrè, Ed., Vol. 2 (Wiley, New York, 1953), Part 1.
11. J. Ise, Jr., R. V. Pyle, D. A. Hicks, and R. M. Main, Rev. Sci. Instr. 25, 437 (1953).
12. S. D. Bloom, E. Reilly, and B. J. Toppel, "A High-Pressure Proportional Counter for Fast Neutron Spectroscopy", BNL-358 (T-66) June 1955.
13. C. B. A. McCosker, J. Sci. Inst. 21, 120 (1944).
14. R. W. P. Drever, A. Moljk, and S. C. Curran, Nuclear Instr. 1, No. 1, 41 (1957).
15. R. Giles, Rev. Sci. Instr. 24, 986 (1953).
16. R. E. Benenson and M. B. Shurman, Rev. Sci. Instr. 29, 1 (1958).
17. S. A. Korff, Electron and Nuclear Counters (Van Nostrand, New York, 1946).
18. J. Sharpe, Nuclear Radiation Detectors (Wiley, New York, 1953).
19. B. B. Benson, Rev. Sci. Instr. 17, 533 (1946).
20. B. T. Price, C. C. Horton, and K. T. Spinney, Radiation Shielding, (Pergamon Press, New York, 1957).
21. B. B. Rossi and H. H. Staub, Ionization Chambers and Counters (McGraw-Hill, New York 1949).
22. W. N. English and G. C. Hanna, Can. J. Phys. 31, 768 (1953).
23. D. R. Corson and R. R. Wilson, Rev. Sci. Instr. 19, 207 (1948).

24. S. C. Curran and S. D. Craggs, Counting Tubes. Theory and Application (Academic Press, New York, 1949).

25. D. H. Wilkinson, Ionization Chambers and Counters (Cambridge University Press. Cambridge, England, 1950).

26. D. West, "Energy Measurements with Proportional Counters" in J. O. Newton and B. Rose, Progress in Nuclear Physics, Vol. 3 (Pergamon Press, New York, 1953).

27. G. C. Hanna and B. Pontecorvo, Phys. Rev. 75, 983 (1949).

28. G. C. Hanna, D. H. W. Kirkwood, and B. Pontecorvo, Phys. Rev. 75, 985 (1949).

29. S. C. Curran, J. Angus, and A. L. Cockroft, Phil. Mag. 40, 36 (1949).

30. J. Angus, A. L. Cockroft, and S.C. Curran, Phil. Mag. 40, 522 (1949).

31. A. L. Cockroft and S.C. Curran, Rev. Sci. Instr. 22, 37 (1951).

32. G. M. Insch and S. C. Curran, Phil. Mag. 42, 892 (1951).

33. L. Colli, Phys. Rev. 95, 892 (1954).

34. W. Finkelburg, Atomic Physics (McGraw-Hill, New York, 1950).

35. R. Meyerott, Phys. Rev. 70, 671 (1946).

36. S. Glasstone and M. C. Edlund, The Elements of Nuclear Reactor Theory (D. Van Nostrand, New York, 1952).

37. Wilmot N. Hess, "Neutrons from (α-n) Sources", UCRL-3839, July 1957.

38. H. A. Bethe, Revs. Modern Phys. 22, 213 (1950).

39. M. S. Livingston and H. A. Bethe, Revs. Modern Phys. 9, 245 (1937).

40. J. O. Hirschfelder and J. L. Magee, Phys. Rev. 73, 207 (1948).

41. A. T. Nelms, "Energy Loss and Range of Electrons and Positrons", NBS Circ. 577 (1956).

42. W. H. Zinn and S. Seely, Phys. Rev. 52, 919 (1937).

43. Lawrence Ruby, "A Suspendable Pulsed Neutron Source", UCRL-3414 May 1956.

44. A. O. Hanson, R. F. Taschek, and J. H. Williams, Revs. Modern Phys. 21, 635 (1949).

45. W. E. Bennett, C. E. Mandeville, and H. T. Richards, Phys. Rev. 69, 418 (1946).

46. E. J. Konopinski and E. Teller, Phys. Rev. 73, 822 (1948).

47. A. E. S. Green, Nuclear Physics (McGraw-Hill, New York, 1955).

48. A. O. Hanson and J. L. McKibben, Phys. Rev. 72, 673 (1947).